OPEN ACCESS Freely available online

PLoS one

Localization of Receptor Site on Insect Sodium Channel for Depressant β-toxin BmK IT2

Huiqiong He[1,2☯], Zhirui Liu[1☯], Bangqian Dong[1], Jianwei Zhang[1], Xueqin Shu[1], Jingjing Zhou[1], Yonghua Ji[1]*

1 Lab of Neuropharmacology and Neurotoxicology, Shanghai University, Shanghai, People's Republic of China, **2** Graduate School of Chinese Academy of Sciences, Shanghai Institute of Physiology, Shanghai Institute of Biological Sciences, Chinese Academy of Sciences, Shanghai, People's Republic of China

Abstract

Background: BmK IT2 is regarded as a receptor site-4 modulator of sodium channels with depressant insect toxicity. It also displays anti-nociceptive and anti-convulsant activities in rat models. In this study, the potency and efficacy of BmK IT2 were for the first time assessed and compared among four sodium channel isoforms expressed in *Xenopus* oocytes. Combined with molecular approach, the receptor site of BmK IT2 was further localized.

Principal Findings: 2 μM BmK IT2 strongly shifted the activation of $DmNa_v1$, the sodium channel from *Drosophila*, to more hyperpolarized potentials; whereas it hardly affected the gating properties of $rNa_v1.2$, $rNa_v1.3$ and $mNa_v1.6$, three mammalian central neuronal sodium channel subtypes. (1) Mutations of Glu_{896}, Leu_{899}, Gly_{904} in extracellular loop Domain II S3–S4 of $DmNa_v1$ abolished the functional action of BmK IT2. (2) BmK IT2-preference for $DmNa_v1$ could be conferred by Domain III. Analysis of subsequent $DmNa_v1$ mutants highlighted the residues in Domain III pore loop, esp. Ile_{1529} was critical for recognition and binding of BmK IT2.

Conclusions/Significance: In this study, BmK IT2 displayed total insect-selectivity. Two binding regions, comprising domains II and III of $DmNa_v1$, play separated but indispensable roles in the interaction with BmK IT2. The insensitivity of $Na_v1.2$, $Na_v1.3$ and $Na_v1.6$ to BmK IT2 suggests other isoforms or mechanism might be involved in the suppressive activity of BmK IT2 in rat pathological models.

Citation: He H, Liu Z, Dong B, Zhang J, Shu X, et al. (2011) Localization of Receptor Site on Insect Sodium Channel for Depressant β-toxin BmK IT2. PLoS ONE 6(1): e14510. doi:10.1371/journal.pone.0014510

Editor: Cameron Neylon, University of Southampton, United Kingdom

Received April 26, 2010; **Accepted** December 5, 2010; **Published** January 14, 2011

Funding: This study was supported by National Basic Research Program of China (2006CB500801 and 2010CB529806) and Key discipline 'Molecular Physiology' of the Shanghai Education Committee. The funders had no role in study design, data collection and analysis, decision to publish, or preparation of the manuscript.

Competing Interests: The authors have declared that no competing interests exist.

* E-mail: yhji@staff.shu.edu.cn

☯ These authors contributed equally to this work.

Introduction

Voltage-gated sodium channels (VGSC) are key membrane proteins responsible for neuron excitability, consisting of an ion-conducting α-subunit accompanied by one or more auxiliary subunits [1]. Generally, the α-subunit comprising four repeated domains (DI–DIV), each containing six transmembrane α-helixes (S1–S6) and a hairpin-like pore loop between S5 and S6 [2], split into an N-terminal part (SS1) and a C-terminal part (SS2). Despite the high structure similarity, various VGSC subtypes display distinct distribution, gating properties and function activities. Some neurotoxins can differentiate among them with preference for certain subtype(s) [3], thus providing clues about the structure-fuction relationship of VGSCs and a potential molecule library for novel drug design or insecticide development.

Amongst the neurotoxins purified from scorpions, β-toxins shift the voltage dependence of VGSC activation to cause subthreshold channel opening, which can be enhanced when channels are preactivated by a depolarizing prepulse [4]. According to the phyletic-bioactivity, the β-toxins may be further divided into: β-mammal toxins, depressant or excitatory insect-specific β-toxins and TsVII-like toxins acting on both mammals and insects [3]. The group of β-toxins is deemed to bind to a common receptor site-4 on VGSC α-subunits, which, however, shows a rather complex picture. The binding sites for β-mammal toxin CssIV (from *Centruroides suffusus suffusus*) and TsVII-like toxin Tz1 (from *Tityus zulianus*) have been mapped to DII S1–S2, DII S3–S4 and DIII SS2-S6 on mammalian VGSCs [4,5,6,7]. The effect of TsVII (i.e. Tsγ from *Tityus serrulatus*) on reducing peak currents are also conferred by the S4 segments of DIII and DIV [8,9]. The excitatory and depressant β-toxins act distinctly, though they both target insect VGSCs [10,11]. DII of $DmNa_v1$ is implicated in the selective recognition of excitatory toxin AahIT (from *Androctonus australis hector*) [12], while several channel regions (DI S5-SS1, DI SS2-S6, DIII SS2-S6, and DIV SS2-S6) may be involved in the interacion with depressant toxin LqhIT2 (from *Leriurus quinquestriatus hebraeus*) [11]. Based on the results of mutation experiments applied on rat VGSCs and information provided by structure analysis of LqhIT2 [13,14], some possible interaction spots in DII S3–S4 of $DmNa_v1$ were deduced. However, no site-directed mutagenesis has been performed on insect VGSC yet as to dissect the receptor site for depressant β-toxins.

BmK IT2, a depressant β-toxin from the scorpion *Buthus martensi* Karsch, can induce strong insect toxicity [15]. Like other

depressant toxins, such as LqhIT2 [11,16], BmK IT2 possesses two non-interacting binding sites (the high/low-affinity binding sites) on insect nerve membranes [17,18]. Despite typical anti-insect features of depressant β-toxins, BmK IT2 displayed antinociceptive and anticonvulsant activities in rat models [19], which were attributed to the specific modulation on brain VGSCs [20]. Such effects against mammals have also been observed in other depressant β-toxins [21,22,23] and explained as a consequence of adaptive evolution of these toxins. However, the binding affinity of BmK IT2 to rat brain synaptosomes was quite low [17,18] and the specific target is still unidentified.

To forward the understanding for the binding features of depressant β-toxins and their intriguing functional diversity, in the present study, we attempted to address the following issues: 1) Can BmK IT2 modulate the mammalian VGSC subtypes from central neuronal system (i.e. $Na_v1.2$, $Na_v1.3$ and $Na_v1.6$)? 2) What is the selectivity of BmK IT2 between these mammal subtypes and insect VGSC $DmNa_v1$? 3) What is the binding/recognition site on insect VGSC for BmK IT2?

Materials and Methods

Materials

BmK IT2 was purified by column chromatography from the crude venom of the Asian scorpion *Buthus martensi* Karsch as described previously [15]. The purity of the toxin was confirmed by mass spectrometry.

The genes encoding the sodium channel α-subunit $DmNa_v1$ (P35500.3) from *Drosophila* paralytic temperature-sensitive and the auxiliary TipE subunit were kindly provided by J. Warmke (Merck, New Jersey, USA) and M. S. Williamson (IACR-Rothamsted, UK), respectively. Plasmids in combination with cDNAs of rat/mouse VGSC α-isoforms i.e. $rNa_v1.2$ (CAA27287), $rNa_v1.3$ (CAA68735) and $mNa_v1.6$ (Q9WTU3.1), as well as β1 subunit were originally from Dr. Alan L. Goldin (University of California, USA).

Construction of channel chimeras and mutants

Five endogenous restriction sites in $rNa_v1.2\alpha$ ORF were used to excise DNA fragments coding for the four channel domains (DI: XhoI/XmaI, DII: XmaI/BglII, DIII: BglII/BstEII, DIV: BstEII/PacI). The parallel DNA fragments of $DmNa_v1$ corresponding to the four parts were amplified by PCR with primers containing restriction sites for XhoI, XmaI, BglII, BstEII and PacI in homologous positions. Four chimeric channels (ChD1, ChD2, ChD3 and ChD4) were generated by introducing four $DmNa_v1$ fragments into excised $rNa_v1.2\alpha$ so that individual domains of $rNa_v1.2\alpha$ were replaced by those of $DmNa_v1$ channel. The exchange of DIII SS2 loops between $DmNa_v1$ and $rNa_v1.2\alpha$ were accomplished with PCR-based mutagenesis, giving rise to two products: L(Dm)$Na_v1.2$ (M_{1425}I, D_{1426}Q, Y_{1429}N, A_{1430}D, V_{1432}I, N_{1436}E, E_{1438}D, L_{1439}K, K_{1442}I, Y_{1443}R, D_{1445}T) and L(1.2)DmNa_v1 (I_{1512}M, Q_{1513}D, N_{1516}Y, D_{1517}A, I_{1519}V, E_{1523}N, D_{1525}E, K_{1526}L, T_{1532}D). L(Dm)$Na_v1.2$ means that the loop from the $DmNa_v1$ as donor was constructed in $rNa_v1.2$ as acceptor and vice versa.

In addition, site-directed mutagenesis was performed to introduce a series of mutations into $DmNa_v1$ and the resulting mutants were as follows: multiple-residue mutant DmM5 (I_{1512}M/Q_{1513}D/N_{1516}Y/D_{1517}A/I_{1519}V), double-residue mutant DmI_{1529}K/R_{1530}Y and single-residue mutants DmD_{838}C, DmE_{896}C, DmL_{899}C, DmG_{904}N, DmE_{1523}N, DmK_{1526}L, DmI_{1529}K and DmR_{1530}Y. Primers were designed with Primer5.0 (PremierBiosoft, USA) (See Table S1). All clones were verified by DNA sequencing according to their wild-type sequences (See Figure S1). Plasmid DNAs were harvested and isolated from XL1-blue E. coli (Stratagene, USA).

Voltage-gated sodium channel expression and Electrophysiological studies

Mammalian VGSCs $rNa_v1.2\alpha$, $rNa_v1.3\alpha$ and $mNa_v1.6\alpha$ were expressed in *Xenopus* oocytes accompanied with auxiliary subunit β1 while the insect VGSC $DmNa_v1$ was coexpressed with TipE for generating robust Na^+ currents.

The genes for wild-type VGSCs, chimeras, mutants and those for the auxiliary subunits (TipE and β1) were transcribed *in vitro* using T7 RNA-polymerase and the mMESSAGE mMACHINE^{TM} system (Ambion, Austin, TX). *Xenopus* laevis oocytes were prepared [24] and injected with 0.5–10 ng of each wild-type cRNA species (1:1 weight mixture respectively for $rNa_v1.2\alpha/\beta1$, $rNa_v1.3\alpha/\beta1$, $mNa_v1.6\alpha/\beta1$ and Para/TipE) or with 35–50 ng of each cRNA from chimeric/mutant channels with β1/TipE cRNA (1:1 weight ratio). Oocytes were incubated at 20°C for 2–5 days in ND96 solution (in mM: NaCl 96, KCl 2, $CaCl_2$ 1.8, $MgCl_2$ 2 and HEPES 5, pH 7.5), supplemented with 5 mM pyruvate and 0.1 mg/ml gentamicin.

Two-electrode voltage-clamp recordings were performed at room temperature (18°–22°C) using the TURBO TEC-03X amplifier (npi Instruments, Germany) and Cellwork E5.5 software (npi electronic Instruments). Voltage and currents electrodes were filled with 3 M KCl. Currents were filtered at 1.3 kHz and sampled at 10 kHz with a four-pole Bessel filter. Bath solution composition was (in mM): NaCl 96, KCl 2, $CaCl_2$ 1.8, $MgCl_2$ 2 and HEPES 5 (pH 7.4). Toxin BmK IT2 were diluted with bath solution and applied directly to the bath at desired concentration.

From a holding potential of −100 mV, oocytes were depolarized with a three-step protocol [25]. The first and last test depolarization of 25 ms duration ranged from −70 mV to +70 mV in steps of 10 mV. The second depolarization (PP) to a voltage of −10 mV was used to prime the channels ensuring maximal binding of the β-toxin to the channel. The third segment of 25 ms at −120 mV ensured recovery from inactivation. Repetition interval was 2 seconds. The peak currents elicited in the test depolarizations were plotted as a function of voltage, resulting in current/conductance-voltage relationships (I/G–V curves). This approach provided an assessment of the BmK IT2 effect on channel activation with and without a depolarizing prepulse (PP) in one experiment.

Data analysis

Data were acquired by Cellworks Reader 3.6 (NPI electronic Instruments) and analyzed with Origin 7.5 (Northampton, USA) software.

Only recordings with leakage below 0.10 μA and fluctuation within 0.05 μA were selected in statistical analysis. The results are shown as means ± SEM with the number of experiments provided as *n* in the talble legends.

Mean conductance (G) was calculated from peak current/voltage relations using the equation $G = I/(V-V_{rev})$, where I is the peak current elicited upon depolarization, V is the membrane potential, and V_{rev} is the reversal potential. The voltage dependence for the activation of I was fit with the Boltzmann relation, $G/G_{max} = 1/[1+\exp(V_{1/2}-V)/k_m]$, where $V_{1/2}$ is the voltage for half-maximum activation and k_m is the slope factor. The EC_{50} values were determined by measuring the currents induced by BmK IT2 at the voltage of channel activation threshold (−40 mV).

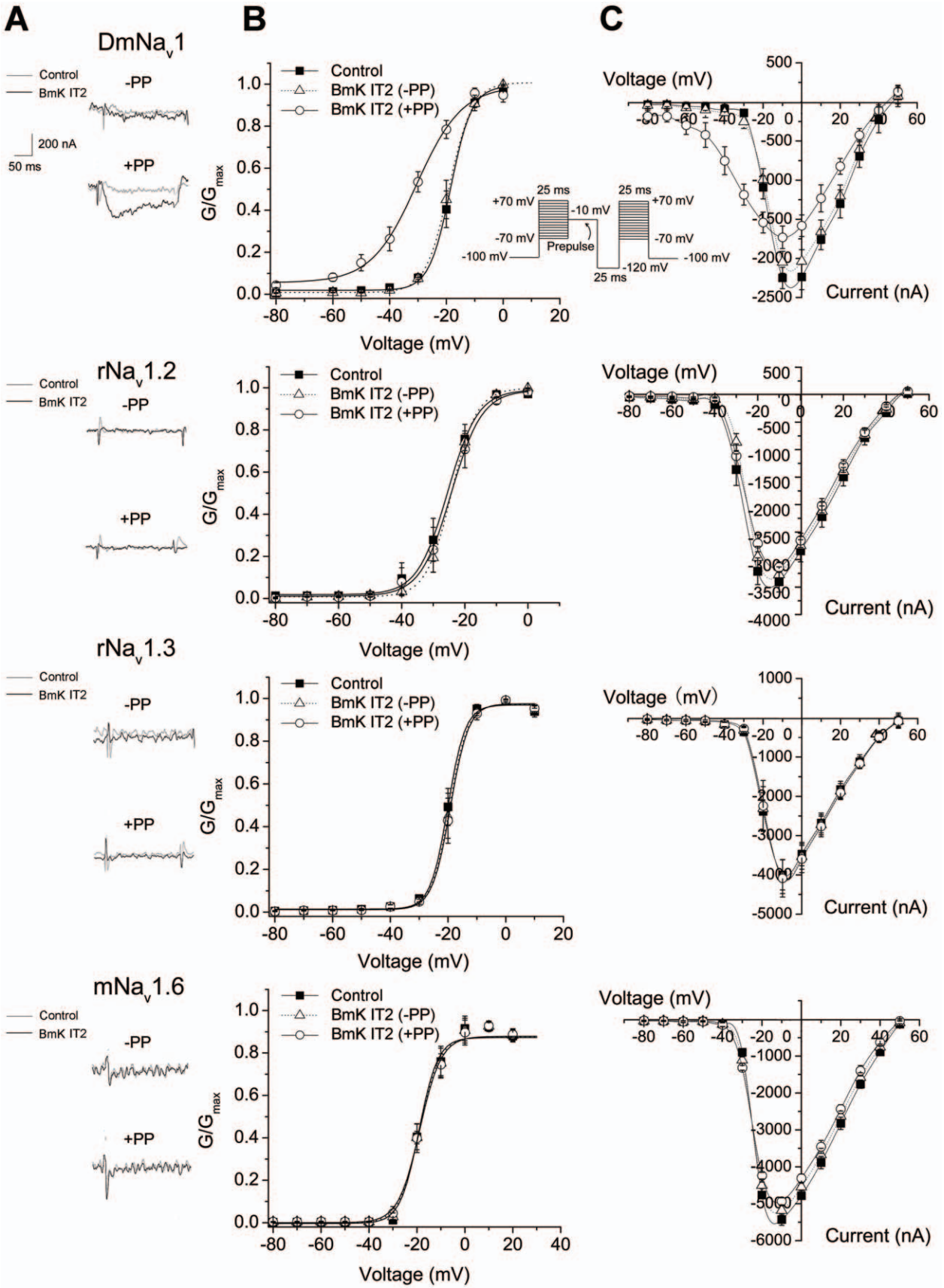

Figure 1. Effect of BmK IT2 on wild-type VGSCs expressed in *Xenopus* oocytes. A. Current responses of rNa$_v$1.2, rNa$_v$1.3, mNa$_v$1.6 and DmNa$_v$1 channels to a test voltage of −50 mV, where channels were closed under control conditions (gray traces). Black traces represented currents

in the presence of 2 μM BmK IT2 without a prepulse (−PP, upper panel) and with a prepulse (+PP, lower panel). The scale bar in figure 1A covered all four embodied currents. B. Normalized conductance plotted as a function of voltage for the indicated channel subtypes. C. Current-voltage curves for the indicated channel types. ■, control conditions; △, 2 μM BmK IT2 without a prepulse (−PP); ○, 2 μM BmK IT2 with a prepulse (+PP).
doi:10.1371/journal.pone.0014510.g001

Results

Efficacy of BmK IT2 on VGSC isoforms from insect and mammalian central neuronal system

Using the two-electrode voltage clamp recording, BmK IT2 was subjected to a comparative study for the effects on four VGSC subtypes, $rNa_v1.2/\beta1$, $rNa_v1.3/\beta1$, $mNa_v1.6/\beta1$ and $DmNa_v1$/TipE expressed in *Xenopus* oocytes (Fig. 1). The voltage-dependent channel activation was investigated by a three-step protocol (see *Materials and Methods*). 2 μM BmK IT2 induced significant subthreshold currents (at −50 mV) in $DmNa_v1$/TipE channels with a depolarizing prepulse (PP) of 25 ms (Fig. 1A). The half-maximal activation voltage ($V_{1/2}$) of $DmNa_v1$/TipE was shifted by about −11 mV and the slope factor (k_m) was increased from 3.72 to 7.97 mV ($p<0.001$, $n=10$) by 2 μM BmK IT2 ($EC_{50}=2.9\pm0.36$ μM, Table 1). This shift was also observed only in the presence of a prepulse (Fig. 1B–C). In contrast, $rNa_v1.2/\beta1$, $rNa_v1.3/\beta1$, $mNa_v1.6/\beta1$ were totally insensitive to BmK IT2 at concentrations of 2 μM (Fig. 1A and B) and even up to 20 μM (Fig. S2). Prolonging the PP duration to 50 ms was unable to enhance the efficacy of BmK IT2 (data not shown). Though the activation of $rNa_v1.3/\beta1$ eventually responded to BmK IT2 at a rather high concentration (50 μM; $\Delta V_{1/2}=-4.84$ mV, data not shown), $rNa_v1.2/\beta1$ and $mNa_v1.6/\beta1$ still remained insensitive. Whether or not β1 subunit was coexpressed with these mammalian VGSC subtypes did not influence the action of BmK IT2 (not shown).

On all investigated VGSC subtypes, a small depression of current amplitude was observed (<10% for mammalian VGSCs and ~20% for $DmNa_v1$/TipE, Fig. 1C) after application of BmK IT2. There were no significant BmK IT2-induced changes in inactivation process of channels (data not shown). The results suggest that BmK IT2 exhibited distinguished subtype selectivity on sodium channels, preferring the insect target rather than mammalian central neuronal isoforms.

Mutations in DII S3–S4 impacted BmK IT2 function on insect VGSC

Previous reports demonstrated that substitutions introduced to DII (e.g. $E_{779}Q$ in DII S1–S2, and $E_{837}Q$, $L_{840}C$, $G_{845}N$ in DII S3–S4 of $rNa_v1.2\alpha$; $G_{658}N$ in DII S3–S4 of $rNa_v1.4$) reduced the effects of the β-toxins Css4 and Tz1 [4,5,6,7]. As for the case of depressant toxin, structural bioinformatics analysis deduced three analogous residues in $DmNa_v1$ (E_{896}, L_{899} and G_{904}) might also be crucial in the interaction with LqhIT2 [13,14]. Based on these studies and considering the high homology between LqhIT2 and BmK IT2, mutations of D_{838}, E_{896}, L_{899} and G_{904} (corresponding to E_{779}, E_{837}, L_{840} and G_{845} in $rNa_v1.2$, Fig. 2A), were individually introduced into $DmNa_v1$.

The mutants were co-expressed with TipE subunit ensuring the functional expression and currents were recorded in the same condition as that of wild type $DmNa_v1$. The gating property of all mutants was not altered with respect to those of wild-type channels, thus the subsequent electrophysiological analysis was not "contaminated" by mutagenesis. The normalized conductance-voltage relationship of mutants were assessed in the absence and presence of 2 μM BmK IT2 with a 25 ms-PP. Mutant $D_{838}C$ showed the similar response to BmK IT2 as wild type $DmNa_v1$ (Fig. 2B), whereas the mutations of Glu_{896}, Leu_{899} and Gly_{904} totally abolished negative shift of voltage-dependent activation induced by 2 μM BmK IT2 ($\Delta V_{1/2}<2.0$ mV, $\Delta k_m<1.0$ mV, $n=7$ or 8, Fig. 2C–E, Table 2). Besides, the mutants $DmE_{896}C$, $DmL_{899}C$ and $DmG_{904}N$ were also resistant to BmK IT2 at higher concentrations (Talbe 1). This result verified that residues E_{896}, L_{899} and G_{904} in DII S3–S4 of $DmNa_v1$ play critical roles in responding to BmK IT2.

DIII from $DmNa_v1$ conferred BmK IT2 sensitivity to $rNa_v1.2$

Although E_{896}, L_{899} and G_{904} positively support the action of BmK IT2, sequence alignments (Fig. 2A) indicate these residues are also conserved in corresponding positions of all BmK IT2-insensitive mammalian VGSCs investigated. It appears that they are necessary, but not sufficient to fulfill the interaction with BmK IT2, suggesting additional channel region(s) might be involved.

To find out the region(s) responsible for BmK IT2 recognition, four chimeras (ChD1, ChD2, ChD3 and ChD4; Fig. 3A) were thus constructed by replacing each domain of $rNa_v1.2\alpha$ with that of $DmNa_v1$ respectively. Current recordings demonstrated that

Table 1. EC_{50} values (μM) of BmK IT2 on wild-type and chimeric/mutated VGSCs.

Channels	EC_{50} (μM)	*n*
$rNa_v1.2$	>50	3
$rNa_v1.3$	>20	4
$mNa_v1.6$	>50	3
$DmNa_v1$	2.9±0.36	5
ChD1	>50	3
ChD2	>50	3
ChD3	22.5±6.65	3
ChD4	>50	3
$DmD_{838}C$	3.6±0.90	3
$DmE_{896}C$	>35	3
$DmL_{899}C$	>35	3
$DmG_{904}N$	>50	3
$L(Dm)Na_v1.2$	ND	/
$L(1.2)DmNa_v1$	ND	/
$DmI_{1529}K/R_{1530}Y$	ND	/
DmM5	ND	/
$DmE_{1523}N$	2.4±0.46	3
$DmD_{1525}E$	3.3±0.73	3
$DmK_{1526}L$	ND	/
$DmI_{1529}K$	15.6±3.60	3
$DmR_{1530}Y$	ND	/
$DmT_{1532}D$	ND	/
$DmI_{1534}L$	ND	/

EC_{50} values (μM) were determined as described in *Methods*. The data were represented as the mean ± SEM and *n* is the number of independent experiments.ND, not determined; /, null.
doi:10.1371/journal.pone.0014510.t001

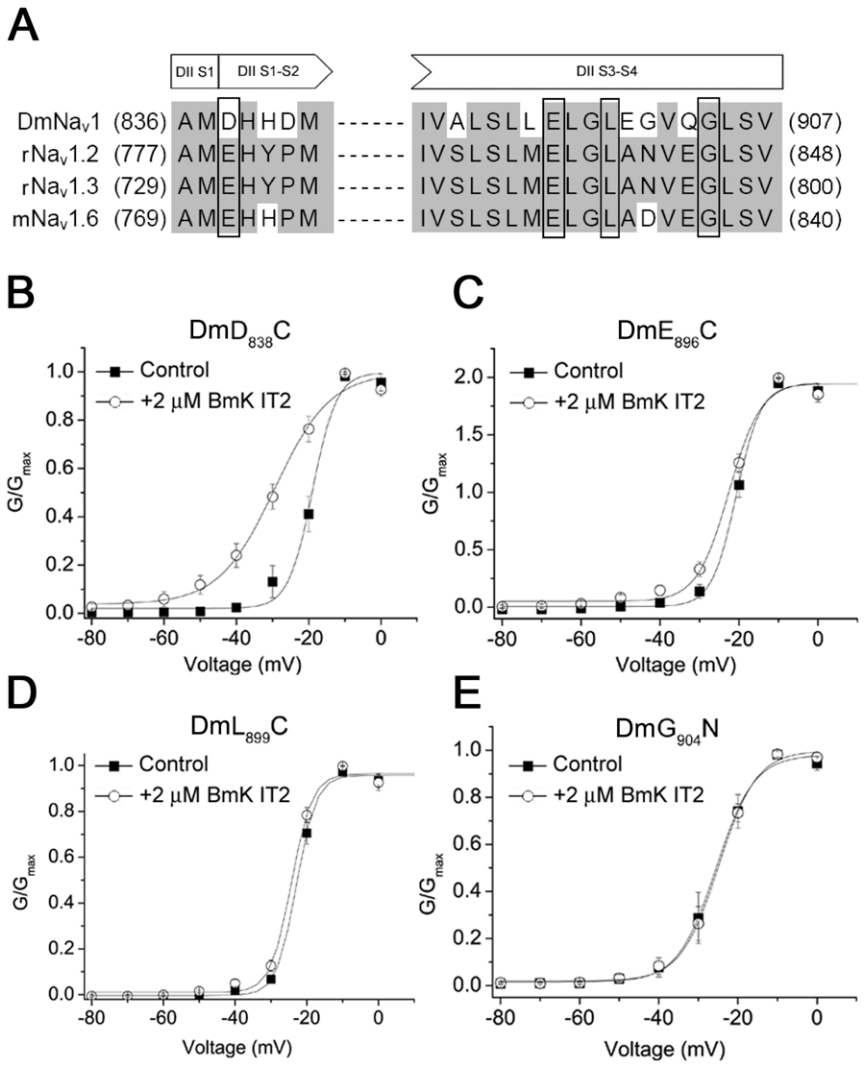

Figure 2. Analysis of mutations in DII of DmNa$_v$1. A. Sequence comparison of extracellular loops DII S1–S2 and DII S3–S4 among wild-type VGSCs. B-E. Normalized conductance-voltage (G–V) curves of DmNa$_v$1 mutants DmD$_{838}$C, DmE$_{896}$C, DmL$_{899}$C and DmG$_{904}$N in the absence (■) and presence (○) of 2 μM BmK IT2. All the currents were recorded after applying a prepulse of −10 mV for 25 ms.
doi:10.1371/journal.pone.0014510.g002

the channel activities were not impaired by cross-species domain substitution. Like rNa$_v$1.2α,most chimeric channels were regulated by mammalian β1 subunit but not TipE from insect (data not shown). The only exception was ChD4 that seemed insensitive to either β1 or TipE.

The activation of chimeras ChD1, ChD2 and ChD4 were hardly modified by 2 μM BmK IT2 (Fig. 3B), like wild type Na$_v$1.2α/β. In contrast, ChD3 gained the response to 2 μM BmK IT2, which caused a statistically significant shift of channel activation ($\Delta V_{1/2} = -5.64$ mV, $p<0.005$, $n = 10$) (Fig. 3B, Table 2). The increased sensitivity in ChD3 ($EC_{50} = 22.5 \pm 6.65$ nM, Table 1) also suggested DIII seemed to play a necessary role in the interaction between insect sodium channel and BmK IT2.

Residues in DIII SS2-S6 critical for the sensitivity of DmNa$_v$1 to BmK IT2

To further clarify the possible interaction site in DIII, a series of mutations have been perfomed in DIII SS2-S6 pore loops of rNa$_v$1.2α and DmNa$_v$1. The mutagenesis design was based on the previous report that suggested DIII SS2-S6 might be involved in the binding of LqhIT2 [11]. First, to verify whether this region accounted for BmK IT2 binding, the DIII SS2 loops were compared (Fig. 4A) and exchanged between DmNa$_v$1 and rNa$_v$1.2 (Fig. 4B), giving rise to two loop chimeras: L(Dm)Na$_v$1.2 and L(1.2)DmNa$_v$1. Unexpectedly, the whole loop replacement in DmNa$_v$1 (I_{1512} to I_{1534}) by that of rNa$_v$1.2 (M_{1425} to L_{1447}) resulted in channels hardly expressed in *Xenopus* oocytes even accompanied by TipE subunit. Thus for generating robust Na^+ currents, two residues in rNa$_v$1.2-type loop had to be restored as present in DmNa$_v$1 (I_{1529}/R_{1530}) (See *Material and Methods*). Double mutant DmI_{1529}K/R_{1530}Y was then produced as the compensation of the incomplete loop substitution.

Similar to the case of chimera ChD3, in the presence of 2 μM BmK IT2 and a 25 ms prepulse, the voltage-dependent activation of L(Dm)Na$_v$1.2 displayed a mild but significant shift with $\Delta V_{1/2}$ of about −5 mV ($p<0.05$, $n = 8$, Fig. 4C and Table 2). As for L(1.2)DmNa$_v$1 (Fig. 4D), the substitution by most part of the DIII SS2 loop from rNa$_v$1.2 could not prevent BmK IT2-induced shift in the voltage of half-maximal activation ($\Delta V_{1/2} = -12.48$ mV).

Table 2. Parameters for the voltage dependent activation of wild-type and chimeric/mutated VGSCs.

Channels	$V_{1/2}$	$V_{1/2}$(+BmK IT2)	$\Delta V_{1/2}$	k_m	k_m(+BmK IT2)	*n*
$rNa_v1.2$	−25.45±0.67	−24.31±0.68	1.14±0.01	4.78±0.54	4.88±0.55	8
$rNa_v1.3$	−20.06±0.32	−19.16±0.36	0.90±0.04	3.03±0.54	3.14±0.50	8
$mNa_v1.6$	−19.14±0.72	−18.82±0.80	0.32±0.08	3.93±0.76	4.48±0.76	8
$DmNa_v1$	−18.52±0.34	−30.44±0.70	−11.92±0.36	3.72±0.40	7.97±0.65	10
ChD1	−20.60±0.32	−20.65±0.28	−0.05±0.04	2.13±0.24	2.33±0.33	10
ChD2	−17.41±0.22	−18.28±0.21	−0.87±0.01	4.82±0.60	4.92±0.49	10
ChD3	−23.40±0.29	−29.04±0.29	−5.64±0.00	3.85±0.25	3.59±0.26	10
ChD4	−20.22±0.39	−21.66±0.41	−1.44±0.02	4.21±0.41	4.40±0.38	10
$DmD_{838}C$	−18.95±0.62	−29.40±0.98	−10.45±0.36	3.33±0.76	7.68±0.88	7
$DmE_{896}C$	−20.68±0.38	−22.54±0.52	−1.86±0.14	3.10±0.57	4.05±0.45	6
$DmL_{899}C$	−22.89±0.38	−24.28±0.39	−1.39±0.01	2.76±0.28	2.90±0.22	7
$DmG_{904}N$	−25.55±0.57	−24.89±0.57	0.66±0.00	4.80±0.46	4.79±0.45	8
$L(Dm)Na_v1.2$	−21.01±0.31	−26.06±0.39	−5.05±0.08	3.71±0.34	4.79±0.32	7
$L(1.2)DmNa_v1$	−21.87±0.64	−34.35±0.72	−12.48±0.08	4.76±0.58	5.48±0.62	9
$DmI_{1529}K/R_{1530}Y$	−24.82±0.48	−29.88±0.48	−5.06±0.00	4.85±0.39	5.05±0.46	8
DmM5	−21.68±0.35	−28.24±0.55	−6.56±0.20	2.85±0.40	5.73±0.49	6
$DmE_{1523}N$	−25.32±0.56	−37.42±0.84	−12.10±0.28	3.90±0.40	6.89±0.75	7
$DmD_{1525}E$	−21.32±0.34	−31.05±0.58	−9.73±0.24	3.32±0.40	6.50±0.52	6
$DmK_{1526}L$	−21.54±0.39	−33.83±0.59	−12.29±0.20	3.70±0.40	5.71±0.51	8
$DmI_{1529}K$	−23.10±0.17	−22.98±0.18	0.12±0.01	3.42±0.13	4.02±0.14	7
$DmR_{1530}Y$	−20.35±0.51	−25.46±0.98	−5.11±0.47	4.03±0.56	7.69±0.85	8
$DmT_{1532}D$	−20.57±0.36	−30.01±0.70	−9.44±0.34	3.46±0.46	7.41±0.64	6
$DmI_{1534}L$	−24.64±0.42	−32.63±0.55	−7.99±0.13	2.96±0.23	5.90±0.45	7

The values of half-maximum activation voltage $V_{1/2}$ and corresponding slope factor (k_m) were determined in the absence and presence of 2 μM BmK IT2. Application of BmK IT2 shifted channel activation by $\Delta V_{1/2}$. The data were represented as the mean ± SEM and *n* is the number of independent experiments.

doi:10.1371/journal.pone.0014510.t002

Interestingly, however, unlike wild type $DmNa_v1$, the slope factor of its activation curve was barely affected by BmK IT2 ($L(1.2)DmNa_v1$: $\Delta k_m < 1$ mV, n = 8; $DmNa_v1$: $\Delta k_m = +4.25$ mV, n = 10; Table 2). It was noticeable that double-mutant $DmI_{1529}K/R_{1530}Y$ exhibited largely attenuated sensitivity to 2 μM BmK IT2 as the toxin-induced $\Delta V_{1/2}$ decreased to −5.06 mV with the slope factor (k_m) unchanged (Table 2). The results indicats that the DIII SS2-S6 pore-loop of $DmNa_v1$ plays a major role in BmK IT2 interaction and it was the main contributor in conferring BmK IT2 sensitivity to $rNa_v1.2$.

To determine the residue(s) in this region critical for the interaction with BmK IT2, a series of site-directed mutations of $DmNa_v1$ were produced (see *Materials and Methods*). All mutants displayed gating parameters (Table 2) similar to those of wild type $DmNa_v1$, ruling out the possibility that the alteration of gating behavior was involved in variation of BmK IT2 sensitivity. Subsequent analysis demonstrated that among all the mutants (Fig. 5), the potency of 2 μM BmK IT2 was obviously decreased on DmM5, $DmI_{1529}K$, $DmR_{1530}Y$ and $DmI_{1529}K/R_{1530}Y$, with respect to wild-type $DmNa_v1$. The alterations in voltage-dependent activation induced by 2 μM BmK IT2 were in the order that ($\Delta V_{1/2}$, Δk_m): $DmNa_v1$ (−11.92 mV, +4.25 mV)>$DmR_{1530}Y$ (−5.11 mV, +3.66 mV), DmM5 (−6.56 mV, +2.88 mV)>$DmI_{1529}K/R_{1530}Y$ (−5.06 mV, +0.20 mV)>$DmI_{1529}K$ (+0.12 mV, +0.60 mV). Notably, mutant $DmI_{1529}K$ was less sensitive to BmK IT2 (EC_{50} = 15.6±3.60 nM, Talbe 1), indicating an especially critical role of residue I_{1529} in the interaction with BmK IT2.

Discussion

VGSC subtype-selectivity of BmK IT2

BmK IT2 was classified into the group of β-depressant insect toxin because: 1) it shares high sequence similarity with other well-defined depressant anti-insect toxins, such as LqhIT2, LqqIT2 and BjIT2 [26]; 2) BmK IT2 is toxic to insect but not mammals [27,28]. This insect-selectivity was also observed in binding experiments tested on cockroach nerve cords which displayed a 200–300 fold higher affinity with BmK IT2 than rat brain synaptosomes [17]. However, like some other depressant β-toxins [21,22,23], BmK IT2 also evolves function against mammals, e.g. antinociceptive and anticonvulsant activities in rat models [19]. As recent studies have mostly focused on the pharmacological phenotype of BmK IT2, the underlying mechanism and molecular target in rat brain remain unintelligible. In this study, the efficacy and selectivity of BmK IT2 was assayed for the first time among independently cloned VGSCs from insect ($DmNa_v1$) and mammalian central nervous system (i.e. $rNa_v1.2$, $rNa_v1.3$ and $mNa_v1.6$) expressed in *Xenopus* oocytes.

Results showed that the main effects of BmK IT2 on $DmNa_v1$ included a decrease of peak Na^+ current (by ~20%) and a significant hyperpolarizing shift of the activation. These are typical effects for scorpion depressant β-toxins. The increase of the slope value of activation curve, reflecting the decreased voltage dependence of activation process and a larger subthreshold channel open probability, is also observed in previous reports

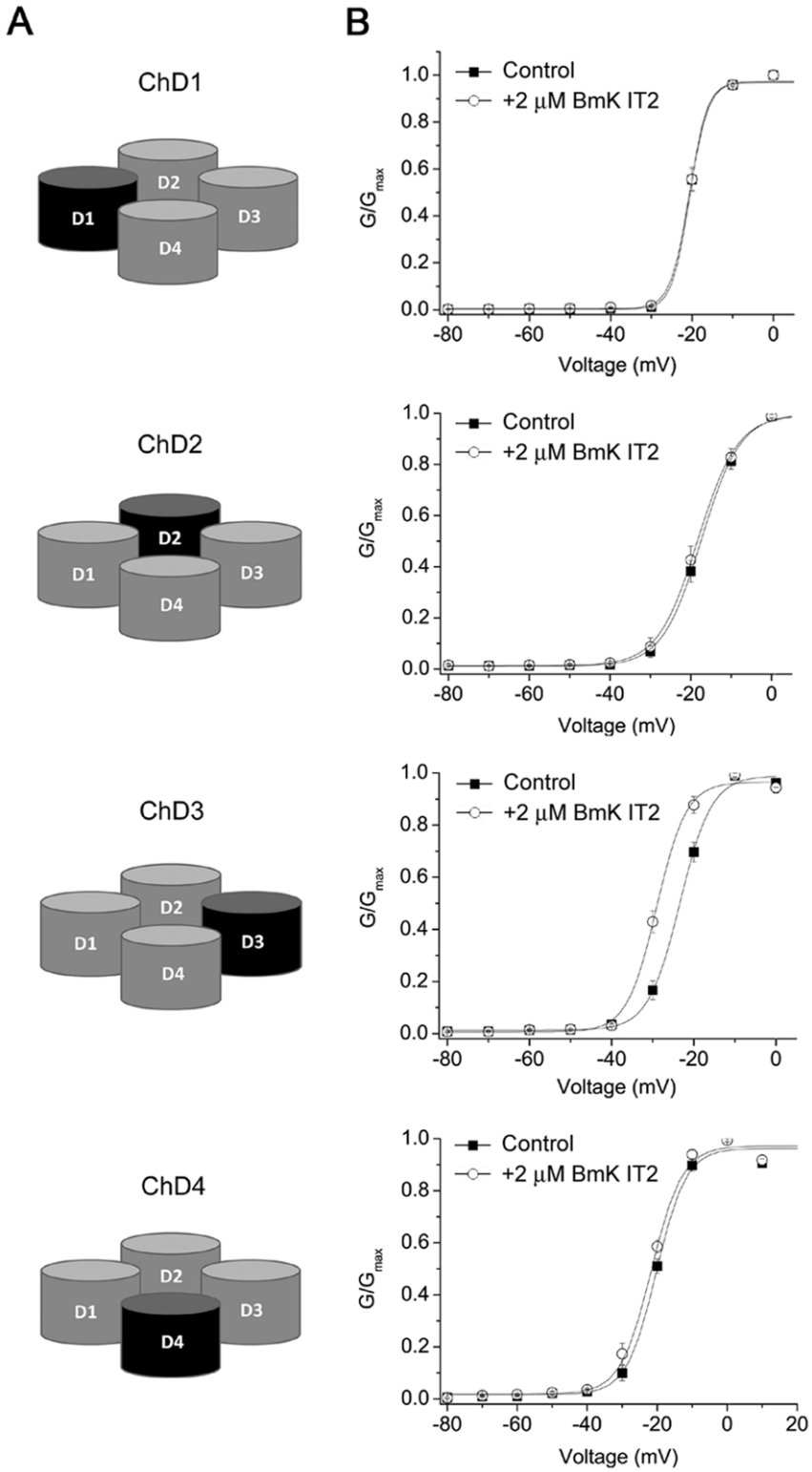

Figure 3. Schematic composition of DmNa$_v$1-Na$_v$1.2 domain chimeras and effect of BmK IT2 on four chimeric channels. A. Cartoons illustrating the construction of channel chimeras. The channel domains of rNa$_v$1.2 were shown in grey, while the domains from DmNa$_v$1 were shown in black. B. Normalized conductance-voltage plotted for chimeras ChD1-ChD4 before (■) and after (○) application of 2 μM BmK IT2, with a prepulse (PP).

doi:10.1371/journal.pone.0014510.g003

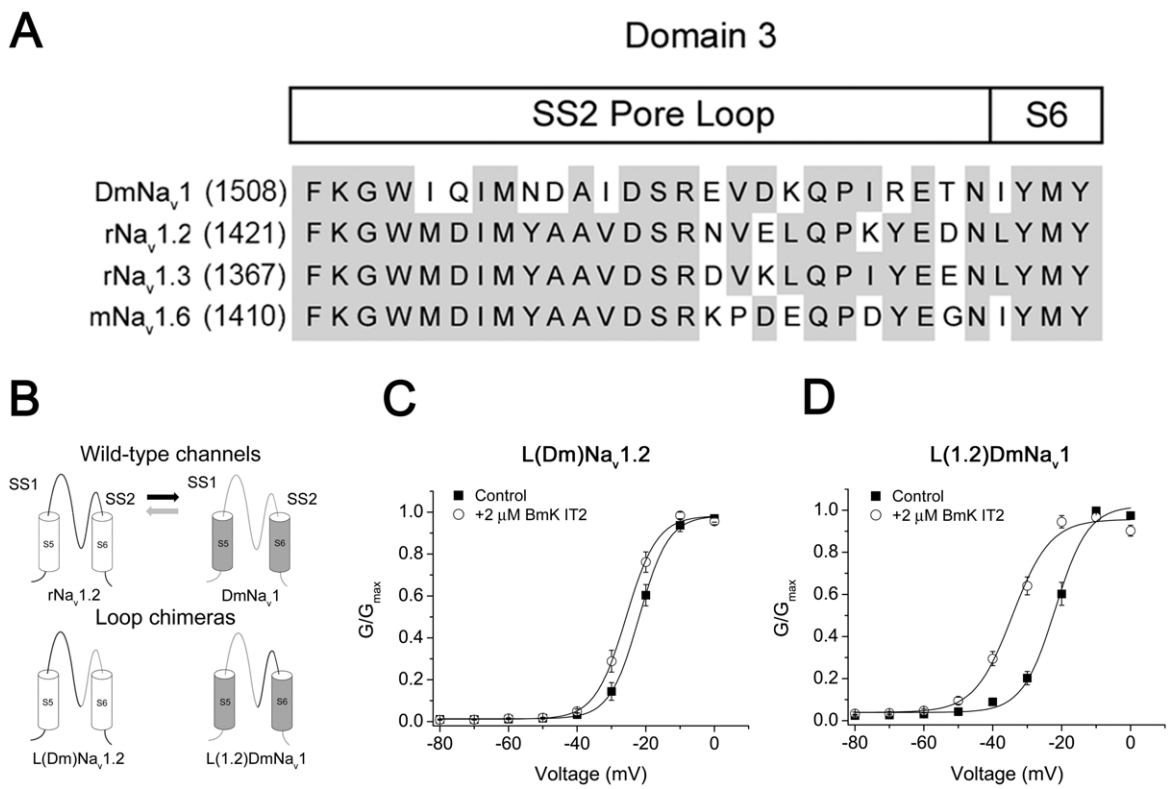

Figure 4. Analysis of DmNa$_v$1-Na$_v$1.2 DIII SS2 loop chimeras. A. Sequences of SS2 loop in DIII of wild-type VGSCs. B. Diagram illustrating the composition of the SS2 loop chimeras L(Dm)Na$_v$1.2 and L(1.2)DmNa$_v$1 (Na$_v$1.2 SS2 loop: grey; DmNa$_v$1 SS2 loop: black). C–D. Effect of BmK IT2 on voltage-dependent activation of L(Dm)Na$_v$1.2 and L(1.2)DmNa$_v$1 with a prepulse (PP) of −10 mV for 25 ms. ■, control conditions; ○, 2 μM BmK IT2.
doi:10.1371/journal.pone.0014510.g004

characterizing the function of depressant β-toxins LqqIT2 and LqhIT2 [29,30].

In contrast, three mammalian VGSCs were totally insensitive to BmK IT2. The low affinity of BmK IT2 to rat brain synaptosomes can be explained by the insensitivities of Na$_v$1.2 and Na$_v$1.6,which are dominant VGSC subtypes spreading throughout CNS [31,32], to BmK IT2. It is noteworthy that BmK IT2 was capable of inhibiting the total Na^+ currents in rat dorsal root ganglion (DRG) neurons [20]. According to our results that Na$_v$1.2, Na$_v$1.3 and Na$_v$1.6 are BmK IT2-insensitive, the action of BmK IT2 on Na^+ currents of DRG neurons may be a result of selective modulation on other neuronal VGSC subtypes, most likely Na$_v$1.7, Na$_v$1.8 and/or Na$_v$1.9 channels. Thus, it may allow us to speculate that peripheral nerve VGSC subtypes might be the major targets responsible for BmK IT2-induced anti-nociception and anti-convulsant effects in rat models, though the subtypes or other membrane proteins that are possibly involved in the working mechanism of BmK IT2 still need to be further characterized.

Construction of insect-mammalian chimeric channels

Since the insect and mammalian VGSCs are highly similar in both structural and functional properties, insect-mammalian chimeras could be constructed to determine the regions responsible for the toxin recognition and interaction. Previously for localizing the insect VGSC domain that binds β-excitatory toxin AahIT, a chimeric channel was constructed from rat brain rNa$_v$1.2 in which DII was replaced by that of *Drosophila* [12]. Here we also chose rNa$_v$1.2 as backbone of chimeric channels that accepted insect VGSC domains considering that: 1) rNa$_v$1.2 channel is insensitive to BmK IT2 at very high concentration (e.g. 20 μM); 2) as a typical VGSC subtype from mammalian nervous system, rNa$_v$1.2 channel has been well characterized in *Xenopus* oocytes and displays an excellent performance in expression level. The four resulting insect-mammalian chimeras were all expressed functionally and identified to be TTX-sensitive VGSCs. Chimeric channels could be regulated by β1 subunit except ChD4 that seemed insensitive to either β1 or TipE subunit. The low current density of ChD4 was improved only by prolonging the expression time duration. These results agreed with the finding that the binding site for β1 was localized to DIV in rNa$_v$1.2 [33] and implicated that TipE might not regulate DmNa$_v$1 through DIV.

To directly reveal the BmK IT2 binding region(s) in DmNa$_v$1 channel and confirm the results obtained in Na$_v$1.2 backbone chimeras, we also attempted to generate the mammalian-insect chimeras in which the independent domains of DmNa$_v$1 were replaced by those of rNa$_v$1.2. Unfortunately, due to the rather low expression level, these chimeras failed to serve as satisfying candidates for the subsequent pharmacological analysis.

The binding feature of BmK IT2 on DmNa$_v$1

The classical voltage-sensor trapping model indicates that β-toxins function as a stablizer of activated state of VGSCs by trapping the outward DII S4 and hereby shift the activation threshold to more hyperpolarized potentials [4].

In this study, mutations of G_{904}, E_{896}, L_{899} in DII S4 of DmNa$_v$1 completely abolished the action of BmK IT2, suggesting that, like other β-toxins (e.g. CssIV and Cn2), BmK IT2 functionally interacts with DmNa$_v$1 through DII S4 as described in the voltage-sensor trapping model (Fig. 6). However, these residues could not serve as a major determinant to BmK IT2

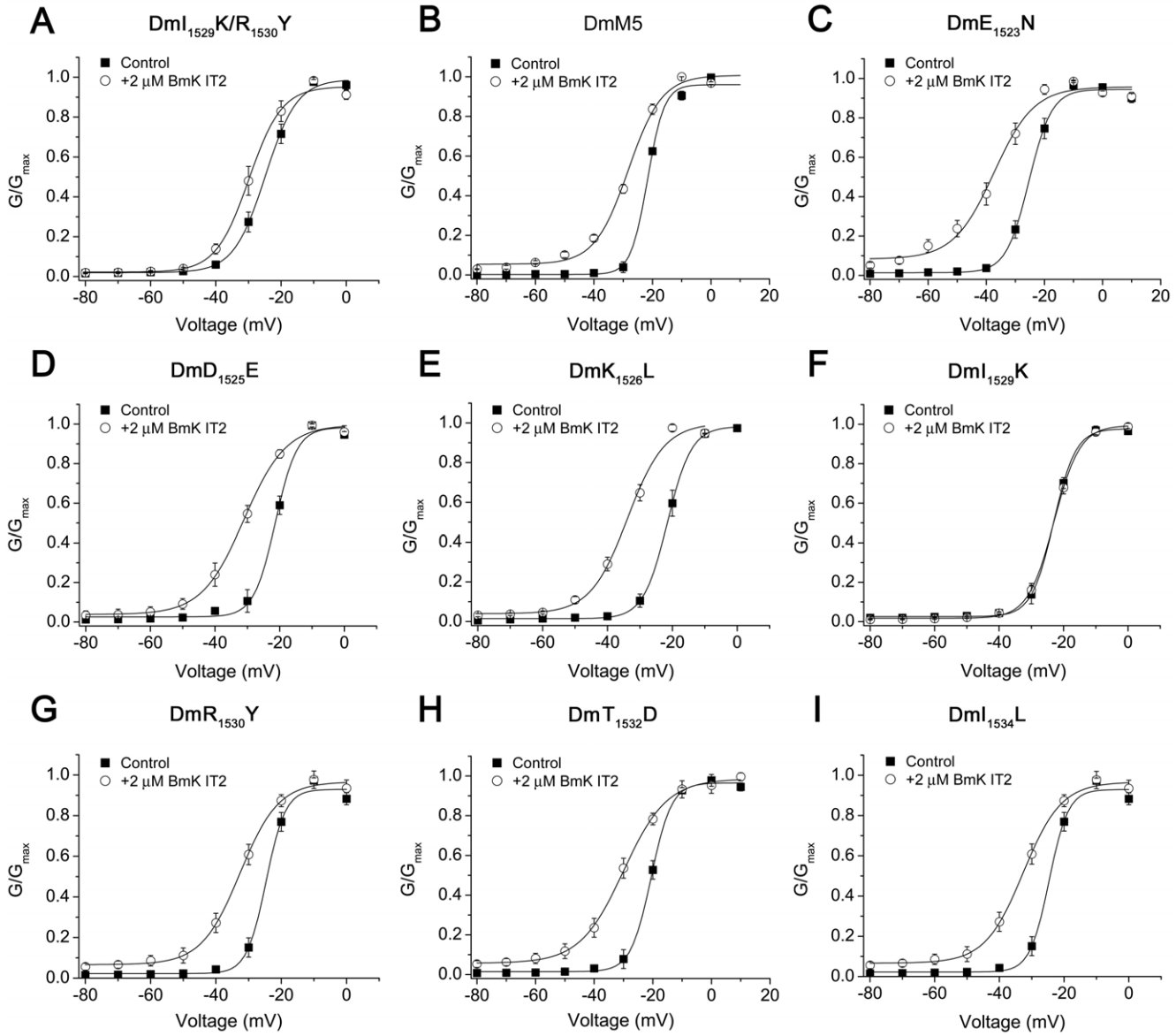

Figure 5. Site-directed mutations introduced in DIII SS2-S6 loop of DmNa$_v$1. A–I. Normalized conductance-voltage curves for the indicated mutant channels before (■) and after (○) application of 2 μM BmK IT2, with a prepulse (+PP) in all cases.
doi:10.1371/journal.pone.0014510.g005

sensitivity as they are well conserved in the BmK IT2-insensitive mammalian channels like rNa$_v$1.2, rNa$_v$1.3 and mNa$_v$1.6. The subsequent study revealed that DIII rather than DII could confer BmK IT2 insect-preference to mammalian sodium channel. The channel epitope that interacts with BmK IT2 was further narrowed down to residues around the N-part of DIII SS2-S6 loop ($I_{1512}/Q_{1513}/N_{1516}/D_{1517}/I_{1519}$) as well as the hydrophobic I_{1529} and the positive R_{1530}, implying the hydrophobic and electrostatic interactions may both be decisive for toxin binding. Although the residue alterations at positions 1512–1526 and at position 1530 had minor impact on toxin efficacy, the exchange of hydrophobic Ile at position 1529 in DmNa$_v$1 to the Lys present in rNa$_v$1.2 largely impaired the toxin-channel interaction. Thus the central role of I_{1529} seemed to support the hydrophobic interaction in toxin-channel inter-recognition (Fig. 6).

Apparently, the receptor site for BmK IT2 involves at least two channel regions: 1) DII S3–S4 linker, for mediating toxin functional interaction with voltage-sensor; 2) DIII SS2 loop: the determinant for BmK IT2 specific targeting.This is different from the case for excitatory β-toxin: the receptor site for AahIT was found to reside mainly in DmNa$_v$1 DII [12]. Our result confirms that the receptor sites for excitatory and depressant β-toxins are not identical on insect VGSC [10,34], however, they have an overlapping region, i.e. DII. That is in concordance with the fact that excitatory toxins can compete with depressant toxins for the high-affinity binding site on insect nerve membrane [11,34].

Interestingly, despite targeting VGSCs from different phyla, the binding features of BmK IT2 and Tz1, a β-like toxin that can strongly affect the activation of muscular Na$_v$ channel but was incapable of affecting the activation of cardiac and peripheral nerve Na$_v$ channels [5], appear very similar: toxins recognize and bind to the pore loop of DIII and then are capable of trapping the outward movement of voltage-sensor in DII, thus lowering the threshold for channel activation.

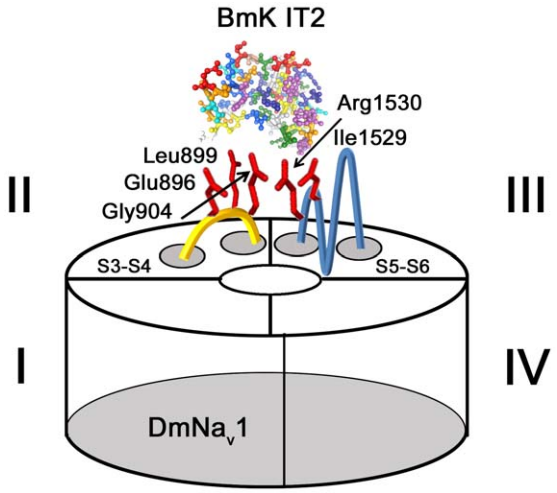

Figure 6. Schematic presentation of domain arrangement and key residues involved in BmK IT2-DmNa$_v$1 interaction. Schematic BmK IT2 structural model (in amino residue) was constructed by Swiss-model Workspace (http://swissmodel.expasy.org) based on the known structure of the depressant β-toxin LqhIT2 (>80% similarity in sequence) (PDB accession 2i61A). Key residues involved in BmK IT2 interaction with DmNa$_v$1 were highlighted in red and indicated with sequence numbers on extracellular loop of DII (yellow) and DIII (blue). doi:10.1371/journal.pone.0014510.g006

Conclusion

The insect-selectivity of BmK IT2 was highlighted in this study when differentiating between heterologously expressed VGSC subtypes from insect and mammalian central nervous system. The results suggested Na$_v$1.2, Na$_v$1.3, and Na$_v$1.6 channels were not involved in mediating the BmK IT2-induced antinociceptive and anticonvulsant effect in rat models. The study revealed the receptor site on insect VGSC DmNa$_v$1 for depressant β-toxin BmK IT2 consisted of at least two regions, i.e. DII and DIII. The recognition epitope for insect-preference were localized to the hydrophobic residues within DIII pore-loop SS2-S6. Finally, the inter-species chimeric channels employed here may provide a promising operation for identifying putative binding site(s) in VGSCs targeted by other specific modulators.

Supporting Information

Figure S1 Sequences of the DmNa$_v$1 mutants indicating the mutated residues in DII and DIII. The loop chimera L(Dm)Na$_v$1.2 was produced by replacing the diversed residues within DIII SS2-S6 loop of rNa$_v$1.2 by those from DmNa$_v$1 (underlined residues) correspondingly. In addition, single- or multiple-mutagenesis were also employed on DmNav1, giving rise to the loop-chimera or mutants listed below. Black dots in loop-chimera/mutants indicated the unchanged residues compared to the sequence of L(Dm)Na$_v$1.2 (or DmNa$_v$1).
Found at: doi:10.1371/journal.pone.0014510.s001 (1.80 MB TIF)

Figure S2 Effect of BmK IT2 on mammalian wild-type VGSCs. Normalized conductance-voltage (G-V) curves of rNa$_v$1.2, rNa$_v$1.3, mNa$_v$1.6 in absence (■) and presence of 20 μM (○) and 50 μM (△) BmK IT2, with a 25 ms prepulse.
Found at: doi:10.1371/journal.pone.0014510.s002 (1.34 MB TIF)

Figure S3 Dose-response curves for effects of BmK IT2 at DmNa$_v$1 and indicated mutants. The EC$_{50}$ values were determined by measuring the currents induced by the toxin at a test pulse of −40 mV (Table 1). The protocol used are shown in the inset.
Found at: doi:10.1371/journal.pone.0014510.s003 (5.03 MB TIF)

Table S1 The localizations of mutated bases are underlined in nucleotide sequence of all the primers. For loop chimeras, the deduced amino acid residues of mutated positions are indicated beneath.
Found at: doi:10.1371/journal.pone.0014510.s004 (0.07 MB DOC)

Acknowledgments

We thank Dr. Alan L. Goldin (University of California, USA) for generous providing of plasmid comprising genes of rNa$_v$1.2α, rNa$_v$1.3α and mNa$_v$1.6α as well as rat β1 subunit. We also appreciate Dr. M. Williamson for kind gift of DmNa$_v$1 and TipE.

Author Contributions

Conceived and designed the experiments: HH YJ. Performed the experiments: HH ZL BD JZ. Analyzed the data: HH ZL. Contributed reagents/materials/analysis tools: JZ XS JZ. Wrote the paper: HH ZL.

References

1. Catterall WA (1992) Cellular and molecular biology of voltage-gated sodium channels. Physiol Rev 72: S15–48.
2. Catterall WA (1995) Structure and function of voltage-gated ion channels. Annu Rev Biochem 64: 493–531.
3. Cestele S, Catterall WA (2000) Molecular mechanisms of neurotoxin action on voltage-gated sodium channels. Biochimie 82: 883–892.
4. Cestele S, Yarov-Yarovoy V, Qu Y, Sampieri F, Scheuer T, et al. (2006) Structure and function of the voltage sensor of sodium channels probed by a beta-scorpion toxin. J Biol Chem 281: 21332–21344.
5. Leipold E, Hansel A, Borges A, Heinemann SH (2006) Subtype specificity of scorpion beta-toxin Tz1 interaction with voltage-gated sodium channels is determined by the pore loop of domain 3. Mol Pharmacol 70: 340–347.
6. Mantegazza M, Cestele S (2005) Beta-scorpion toxin effects suggest electrostatic interactions in domain II of voltage-dependent sodium channels. J Physiol 568: 13–30.
7. Cohen L, Ilan N, Gur M, Stuhmer W, Gordon D, et al. (2007) Design of a specific activator for skeletal muscle sodium channels uncovers channel architecture. J Biol Chem 282: 29424–29430.
8. Bosmans F, Martin-Eauclaire MF, Swartz KJ (2008) Deconstructing voltage sensor function and pharmacology in sodium channels. Nature 456: 202–208.
9. Marcotte P, Chen LQ, Kallen RG, Chahine M (1997) Effects of Tityus serrulatus scorpion toxin gamma on voltage-gated Na+ channels. Circ Res 80: 363–369.
10. Moskowitz H, Herrmann R, Zlotkin E, Gordon D (1994) Variability among insect sodium channels revealed by binding of selective neurotoxins. Insect Biochem Mol Biol 24: 13–19.
11. Gordon D, Moskowitz H, Eitan M, Warner C, Catterall WA, et al. (1992) Localization of receptor sites for insect-selective toxins on sodium channels by site-directed antibodies. Biochemistry 31: 7622–7628.
12. Shichor I, Zlotkin E, Ilan N, Chikashvili D, Stuhmer W, et al. (2002) Domain 2 of Drosophila para voltage-gated sodium channel confers insect properties to a rat brain channel. J Neurosci 22: 4364–4371.
13. Karbat I, Turkov M, Cohen L, Kahn R, Gordon D, et al. (2007) X-ray structure and mutagenesis of the scorpion depressant toxin LqhIT2 reveals key determinants crucial for activity and anti-insect selectivity. J Mol Biol 366: 586–601.
14. Tian C, Yuan Y, Zhu S (2008) Positively selected sites of scorpion depressant toxins: possible roles in toxin functional divergence. Toxicon 51: 555–562.
15. Ji YH, Hattori H, Xu K, Terakawa S (1994) Molecular characteristics of four new depressant insect neurotoxins purified from venom of Buthus martensi Karsch by HPLC. Sci China B 37: 955–963.
16. Cohen L, Gilles N, Karbat I, Ilan N, Gordon D, et al. (2006) Direct evidence that receptor site-4 of sodium channel gating modifiers is not dipped in the phospholipid bilayer of neuronal membranes. J Biol Chem 281: 20673–20679.
17. Li YJ, Tan ZY, Ji YH (2000) The binding of BmK IT2, a depressant insect-selective scorpion toxin on mammal and insect sodium channels. Neurosci Res 38: 257–264.

18. Chai ZF, Bai ZT, Liu T, Pang XY, Ji YH (2006) The binding of BmK IT2 on mammal and insect sodium channels by surface plasmon resonance assay. Pharmacol Res 54: 85–90.
19. Zhao R, Zhang XY, Yang J, Weng CC, Jiang LL, et al. (2008) Anticonvulsant effect of BmK IT2, a sodium channel-specific neurotoxin, in rat models of epilepsy. Br J Pharmacol 154: 1116–1124.
20. Tan ZY, Xiao H, Mao X, Wang CY, Zhao ZQ, et al. (2001) The inhibitory effects of BmK IT2, a scorpion neurotoxin on rat nociceptive flexion reflex and a possible mechanism for modulating voltage-gated Na(+) channels. Neuropharmacology 40: 352–357.
21. Cohen L, Troub Y, Turkov M, Gilles N, Ilan N, et al. (2007) Mammalian skeletal muscle voltage-gated sodium channels are affected by scorpion depressant "insect-selective" toxins when preconditioned. Mol Pharmacol 72: 1220–1227.
22. Peng F, Zeng XC, He XH, Pu J, Li WX, et al. (2002) Molecular cloning and functional expression of a gene encoding an antiarrhythmia peptide derived from the scorpion toxin. Eur J Biochem 269: 4468–4475.
23. Borchani L, Mansuelle P, Stankiewicz M, Grolleau F, Cestele S, et al. (1996) A new scorpion venom toxin paralytic to insects that affects Na+ channel activation. Purification, structure, antigenicity and mode of action. Eur J Biochem 241: 525–532.
24. Goldin AL (1991) Expression of ion channels by injection of mRNA into Xenopus oocytes. Methods Cell Biol 36: 487–509.
25. Borges A, Alfonzo MJ, Garcia CC, Winand NJ, Leipold E, et al. (2004) Isolation, molecular cloning and functional characterization of a novel beta-toxin from the Venezuelan scorpion, Tityus zulianus. Toxicon 43: 671–684.
26. De Lima ME, Figueiredo SG, Pimenta AM, Santos DM, Borges MH, et al. (2007) Peptides of arachnid venoms with insecticidal activity targeting sodium channels. Comp Biochem Physiol C Toxicol Pharmacol 146: 264–279.
27. Ji YHH, Xu H, Terakawa K, S (1994) Molecular characteristics of four new depressant insect neurotoxins purified from venom of Buthus martensi Karsch by HPLC. Sci China B 37: 955–963.
28. Ji YHT, Xu S, K (1994) Primary structure of a depressant insect-selective toxin from venom of scorpion *Buthus martensi* Karsch(*English version*). Chin Sci Bull 39: 945–949.
29. Bosmans F, Martin-Eauclaire MF, Tytgat J (2005) The depressant scorpion neurotoxin LqqIT2 selectively modulates the insect voltage-gated sodium channel. Toxicon 45: 501–507.
30. Gordon D, Ilan N, Zilberberg N, Gilles N, Urbach D, et al. (2003) An 'Old World' scorpion beta-toxin that recognizes both insect and mammalian sodium channels. Eur J Biochem 270: 2663–2670.
31. Beckh S, Noda M, Lubbert H, Numa S (1989) Differential regulation of three sodium channel messenger RNAs in the rat central nervous system during development. EMBO J 8: 3611–3616.
32. Felts PA, Yokoyama S, Dib-Hajj S, Black JA, Waxman SG (1997) Sodium channel alpha-subunit mRNAs I, II, III, NaG, Na6 and hNE (PN1): different expression patterns in developing rat nervous system. Brain Res Mol Brain Res 45: 71–82.
33. Qu Y, Rogers JC, Chen SF, McCormick KA, Scheuer T, et al. (1999) Functional roles of the extracellular segments of the sodium channel alpha subunit in voltage-dependent gating and modulation by beta1 subunits. J Biol Chem 274: 32647–32654.
34. Cestele S, Kopeyan C, Oughideni R, Mansuelle P, Granier C, et al. (1997) Biochemical and pharmacological characterization of a depressant insect toxin from the venom of the scorpion Buthacus arenicola. Eur J Biochem 243: 93–99.